Pergamon

Int. J. Heat Mass Transfer. Vol. 37, No. 5, pp. 855–864, 1994

0017-9310/94 $6.00 + 0.00

Heat transfer from polygonal horizontal isothermal surfaces

WITOLD M. LEWANDOWSKI, PIOTR KUBSKI and HENRYK BIESZK

Department of Chemical Engineering, Technical University of Gdańsk,
ul. Majakowskiego 11/12, 80-952 Gdańsk, Poland

(*Received* 15 *January* 1993 *and in final form* 8 *July* 1993)

Abstract—Each regular surface can be considered as a sum of isosceles triangles of different apex angle (ε). Triangular, square, hexagonal and circular plates consist of three, four, six and an unlimited number of triangles of apex angles $\varepsilon = \pi/3$, $\pi/4$, $\pi/6$ and $\Rightarrow 0°$, respectively. Simplified theoretical consideration for extracted repeated fragments of the surface, describing it in the form of triangles, suitable for any polygon, has been performed. Two models of fluid flow over heated surfaces are proposed. The fluid flow direction in the first model was perpendicular to the leading edge and stream lines are parallel to each other. In the second one it has been assumed that fluid flows from the leading edge concentrically towards the apex angle of the considered triangular surface. In both models free boundary layers transform into plumes above the center of the plates. The solutions of these models are presented in the form of dimensionless Nusselt–Rayleigh relations with the function of apex angles as a polygon parameter. The results of experimental investigations of horizontal isothermal triangular, square, hexagonal and circular plates are presented. The free convection heat transfer experiments and visualization were carried out using plates of the same diameter $d = 0.07$ m of the circle inscribed in polygon and glycerine as the test fluid.

INTRODUCTION

FREE CONVECTIVE flow above the upward-facing horizontal surfaces is interesting for industrial applications, hence many papers have been published on this subject [1–9]. However, almost all of them have treated only the cases of horizontal semi-infinite plates [1–5] or sometimes rectangular and circular plates of finite dimensions [6–9]. In many practical applications configurations of heated or cooling surfaces other than those mentioned above exist.

This work is a summary of investigations carried out by the authors concerned with convective heat transfer from polygonal surfaces [10–12].

MODELS OF FREE CONVECTION FROM POLYGONS

The analysis of convective fluid flow above a square, rectangle and disk expressed by Al-Arabi and El-Riedy in ref. [6] in the form of stream lines gives evidence that the boundary layer forms at all circumferential edges (leading edges) and fluid flows perpendicularly to edges and parallel to themselves. This pattern of fluid flow is presented schematically in Fig. 1(a) and it is called the parallel model of free convection heat transfer. This model of fluid flow is valid for most of the plate shapes (triangular, square, rectangular, pentagonal, hexagonal...). The exception to the rule is the fluid pattern above a round horizontal plate. In this case fluid flows not parallel to themselves but concentrically.

By the analogy the model of concentrical fluid flow can also be valid for the other configuration of plate shapes. This flow pattern, proposed for consideration, is shown in Fig. 1(b) and it is called a concentrical model of free convective heat transfer. In Fig. 1 the change of the magnitude of polygon surfaces in relation to the characteristic dimension used is shown. The constant diameter of the circle inscribed in polygons ($d = \text{const.}$) is in Fig. 1(a) and the diameter ($D = \text{const.}$) of the circle circumscribed on polygons is also indicated (Fig. 1(b)). This method of assumption of the characteristic length has no influence on the phenomenon mechanism.

Boundary layer transformation into buoyant plumes, in the first model, take place above bisecting lines. Next, plumes join together above the center of the plate. In the second model, boundary layer transforms above the center of the plate into the plume. The center line of these axially symmetric plumes in these two models are perpendicular to the surface and overlap with the center points of all polygons considered.

From the analysis of flow patterns presented in Fig. 1 it is obvious, that each regular polygon can be considered as a sum of triangles of characteristic apex angles (ε). Triangular, square, pentagonal, hexagonal and circular plates consist of three, four, five, six and an unlimited number of triangles of apex angles $\varepsilon = \pi/3$, $\pi/4$, $\pi/5$, $\pi/6$ and $\Rightarrow 0$, respectively.

It has been assumed that the phenomenon of convective heat transfer can be considered on a representative element of the whole polygonal surface, instead of the whole surface. The solution obtained in the form of the mean value of heat transfer coefficient for triangular fragment of the plate is valid for the whole polygon.

NOMENCLATURE

a	thermal diffusivity, $\lambda/(c_p\rho)$
a	characteristic length, $A/P = D/4$
A	area of heated plate
A	cross-sectional area in boundary layer
A_k	control surface of heating surface
c_p	specific heat at constant pressure of the fluid
C_D, C_d	coefficients
d	diameter of the circle inscribed in the polygon
D	diameter of the circle circumscribed on the polygon
g	gravitational acceleration
h	thickness of the bakelite between copper plates
i	specific enthalpy
L	characteristic length, $D/2$
m	mass flux
Nu_D, Nu_d	Nusselt numbers, $\alpha D/\lambda$, $\alpha d/\lambda$
P	perimeter of the heated plate
Q	heat flux
r	radius of inscribed circle
R	radius of circumscribed circle
$R1$	modified radius considered on surface S (Fig. 3), $R\cdot\cos(\varepsilon/2)/\cos(\varepsilon/2-\phi)$
Ra_D	Rayleigh number, $g\beta\Delta TD^3/(va)$
Ra_R	Rayleigh number, $g\beta\Delta TR^3/(va)$
Ra_d	Rayleigh number, $g\beta\Delta Td^3/(va)$
S	surface of isosceles triangle separated from regular polygon
T	temperature
W	velocity
x	length of the boundary layer
x	horizontal coordinate to the surface
$x1$	boundary of integration of equation (17), $R\cdot\cos(\varepsilon/2)+x\cdot\operatorname{ctg}(\varepsilon/2)$
y	vertical coordinate to the surface
z	horizontal coordinate to the surface
$z1$	boundary of integration of equation (17), $R\cdot\sin(\varepsilon/2)$.

Greek symbols

α	heat transfer coefficient
β	coefficient of volumetric expansion
δ	thickness of boundary layer
Δ	difference
ε	apex angle of the triangle
θ	dimensionless temperature
λ	thermal conductivity
ν	kinematic viscosity
ρ	fluid density
ϕ	angle.

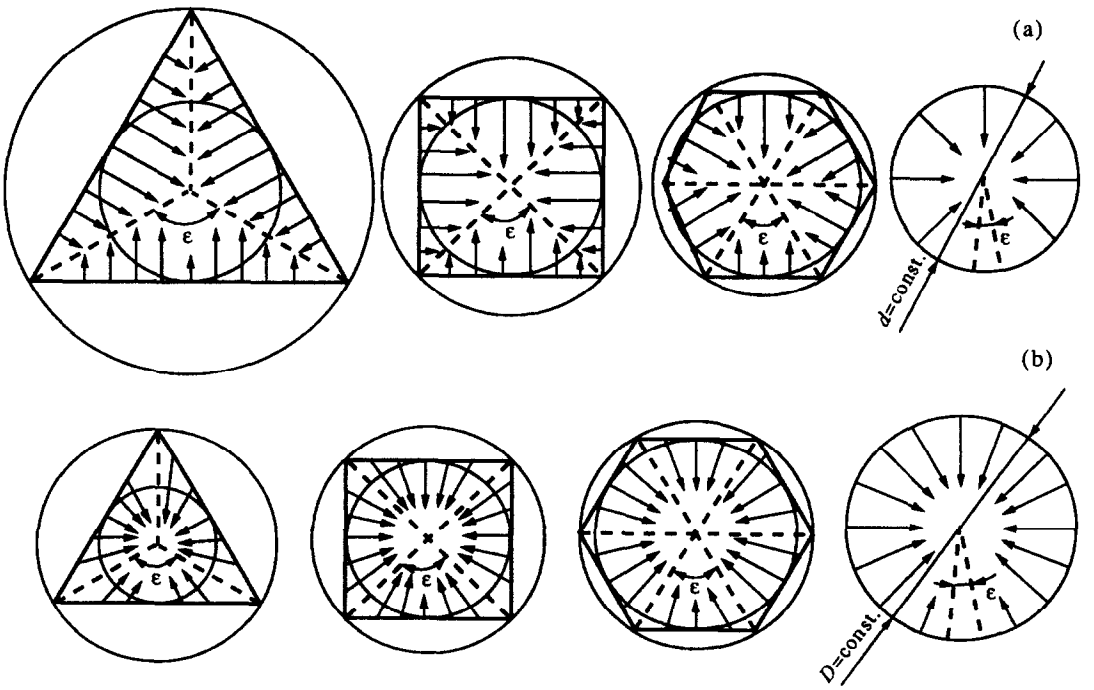

FIG. 1. Theoretical models of convective flow patterns above heated plates of different shapes: (a) with parallel stream lines, (b) with concentric stream lines.

SIMPLIFIED ANALYTICAL SOLUTION

The solution presented below is based on the velocity of the fluid flow calculated for the plane flow pattern (ref. [9, equation (2)]) with simplifying assumptions typical for free convection: the fluid is incompressible and the flow is laminar; inertia forces may be ignored in comparison with the viscous forces; in the boundary layer region, above a triangular element of polygon $W_x \gg W_y$; the physical properties of the fluid in the boundary layer and in the undisturbed region are constant; temperature of the surface (T_w) is constant; thicknesses of thermal and hydraulic boundary layers are the same; the temperature profile in the boundary layer is described not by the direct form of Fourier–Kirchhoff equation, but by

$$\theta = (T_x - T_\infty)/(T_w - T_\infty) = (1 - y/\delta)^2. \quad (1)$$

The quasi-analytical solution of Navier–Stokes equations with dependence (1), presented in ref. [9] in the form of the local and mean velocity in the boundary layer, for horizontal isothermal surface is

$$W_x = \frac{g \cdot \beta \cdot \Delta T}{\nu} \cdot \left(\frac{y^4}{12\delta^2} - \frac{y^5}{30\delta^3} - \frac{y^2}{6} + \frac{7\delta y}{60} \right) \cdot \frac{\mathrm{d}\delta}{\mathrm{d}x}, \quad (2)$$

$$\bar{W}_x = \frac{1}{\delta} \cdot \int_0^\delta W_x \cdot \mathrm{d}y = \frac{g \cdot \beta \cdot \Delta T \cdot \delta^2}{72\nu} \cdot \frac{\mathrm{d}\delta}{\mathrm{d}x}, \quad (3)$$

where $(\mathrm{d}\delta/\mathrm{d}x)$ is the increase of the boundary layer thickness along the path of its growth.

The change in mass flow intensity is

$$\mathrm{d}m = \mathrm{d}(A \cdot \bar{W}_x \cdot \rho), \quad (4)$$

where A is the cross-sectional area of the boundary layer.

The amount of heat necessary to create this change in mass flux is

$$\mathrm{d}Q = \Delta i \cdot \mathrm{d}m = \rho \cdot c_p \cdot \overline{(T_x - T_\infty)} \cdot \mathrm{d}(A \cdot \bar{W}_x). \quad (5)$$

Substitution of the mean value of the temperature

$$\overline{(T_x - T_\infty)} = \frac{1}{\delta} \cdot \int_0^\delta \Delta T \cdot \left(1 - \frac{y}{\delta}\right)^2 \cdot \mathrm{d}y = \frac{\Delta T}{3}, \quad (6)$$

gives

$$\mathrm{d}Q = 1/3 \cdot \rho \cdot c_p \cdot \Delta T \cdot \mathrm{d}(A \cdot \bar{W}_x). \quad (7)$$

The heat flux described by equation (7) may be compared to the heat flux determined by Newton's equation (8):

$$\mathrm{d}Q = \alpha \cdot \Delta T \cdot \mathrm{d}A_k = -\lambda \cdot \left(\frac{\partial \theta}{\partial y}\right)_{y=0} \cdot \Delta T \cdot \mathrm{d}A_k, \quad (8)$$

where A_k is the control surface of the heating plate.

From simplifying assumption of the temperature profile inside the boundary layer (1), the dimensionless temperature gradient on the heated surface may be evaluated as

$$\left(\frac{\partial \theta}{\partial y}\right)_{y=0} = -\frac{2}{\delta}. \quad (9)$$

Substituting equation (9) into equation (8) and equating the result with equation (7), one obtains dependence (10)

$$\tfrac{1}{6} \cdot \rho \cdot c_p \cdot \delta \cdot \mathrm{d}(A \cdot \bar{W}_x) = \mathrm{d}A_k. \quad (10)$$

Substitution of equation (3) in equation (10) gives

$$\delta \cdot \mathrm{d}(A \cdot \delta^2 \cdot \mathrm{d}\delta/\mathrm{d}x) = \frac{432 \cdot \nu \cdot a}{g \cdot \beta \cdot \Delta T} \cdot \mathrm{d}A_k. \quad (11)$$

With the radius (R) of the circle circumscribing the polygon as the characteristic dimension the Rayleigh number is given by

$$Ra = \frac{g \cdot \beta \cdot \Delta T \cdot R^3}{\nu \cdot a}. \quad (12)$$

Substituting equation (12) in equation (11) one obtains:

$$\delta \cdot \mathrm{d}(A \cdot \delta^2 \cdot \mathrm{d}\delta/\mathrm{d}x) = \frac{432 \cdot R^3}{Ra} \cdot \mathrm{d}A_k. \quad (13)$$

Solution of the nonlinear equation (13) depends on the assumed model of the fluid flow and it is different for each model.

MODEL WITH PARALLEL STREAM LINES

In this model (as one can see in Fig. 2), the flow is one-dimensional and plane, so the cross-sectional area and the control surface are ($A = \mathrm{d}z \cdot \delta$) and ($\mathrm{d}A_k = \mathrm{d}z \cdot \mathrm{d}x$) implying that equation (13) has the form:

$$\delta \cdot \mathrm{d}(\delta^3 \cdot \mathrm{d}\delta/\mathrm{d}x) = \frac{432 \cdot R^3}{Ra} \cdot \mathrm{d}x. \quad (14)$$

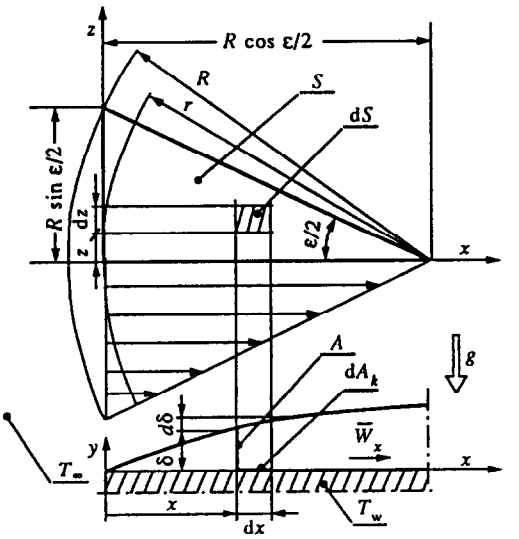

FIG. 2. Physical parallel model of convective heat transfer from a fragment of triangular form of considered heated isothermal surface.

The solution of equation (14), see Appendix A, is

$$\delta = \frac{4.478}{Ra^{1/5}} \cdot x^{2/5} \cdot R^{3/5}. \quad (15)$$

The value of heat transfer coefficients may be determined from equations (8) and (9) as

$$\alpha = \frac{2\lambda}{\delta}. \quad (16)$$

The mean value of heat transfer coefficient is

$$\bar{\alpha} = \frac{1}{S}\int_S \alpha \cdot dS = \frac{4}{R^2 \sin(\varepsilon)} \int_0^{z1} \int_0^{x1} \frac{2\lambda}{\delta} \cdot dx \cdot dz, \quad (17)$$

where boundaries of integration are: $x1 = R \cdot \cos(\varepsilon/2) - x \cdot \mathrm{ctg}(\varepsilon/2)$ and $z1 = R \cdot \cos(\varepsilon/2)$.

By substitution of (15) in equation (17) the Nusselt–Rayleigh relation for the convective heat transfer for an isothermal horizontal polygon is obtained

$$Nu_R = \frac{0.930}{\cos^{2/5}(\varepsilon/2)} \cdot Ra_R^{1/5} \quad \text{or}$$

$$Nu_D = \frac{1.228}{\cos^{2/5}(\varepsilon/2)} \cdot Ra_D^{1/5}. \quad (18)$$

Relation (18) is the solution obtained for assumed parallel fluid flow describing free convective heat transfer from any horizontal, isothermal and regular polygon. For the limiting case of regular polygon—round horizontal plate ($\varepsilon \Rightarrow 0$)—the solution (18) has the form

$$Nu_R = 0.930 Ra_R^{1/5} \quad \text{or} \quad Nu_D = 1.228 Ra_D^{1/5}. \quad (19)$$

MODEL WITH CONCENTRIC STREAM LINES

In this model with concentric stream lines (see Fig. 3) the cross-sectional area and the control surface are $A = r \cdot \delta \cdot d\varepsilon$ and $dA_k = r \cdot dr \cdot d\varepsilon$, respectively, and equation (13) has the form:

$$\frac{\delta}{r} \cdot \frac{d}{dr} \cdot [r \cdot \delta^3 \cdot (-d\delta/dr)] = \frac{432 \cdot R^3}{Ra}. \quad (20)$$

The solution of nonlinear equation (20), presented in Appendix B, has the form

$$\delta = \frac{2.457 \cdot R^{3/4}}{Ra^{1/5}} \cdot \frac{(R1^{7/3} - r^{7/3})^{1/4}}{r^{1/3}}, \quad (21)$$

where $R1 = R \cdot \cos(\varepsilon/2)/\cos(\varepsilon/2 - \phi)$ is the modified, from circle to triangle, radius of the surface considered (S).

The mean value of heat transfer coefficient is

$$\bar{\alpha} = \frac{1}{S}\int_S \alpha \cdot dS = \frac{4}{R^2 \sin(\varepsilon)} \int_0^{\varepsilon/2} \int_0^{R1} \frac{2 \cdot \lambda}{\delta} \cdot r \cdot dr \cdot d\phi. \quad (22)$$

By substitution of dependence (21) to equation (22) the Nusselt–Rayleigh relation for the convective heat transfer from an isothermal horizontal polygon is obtained

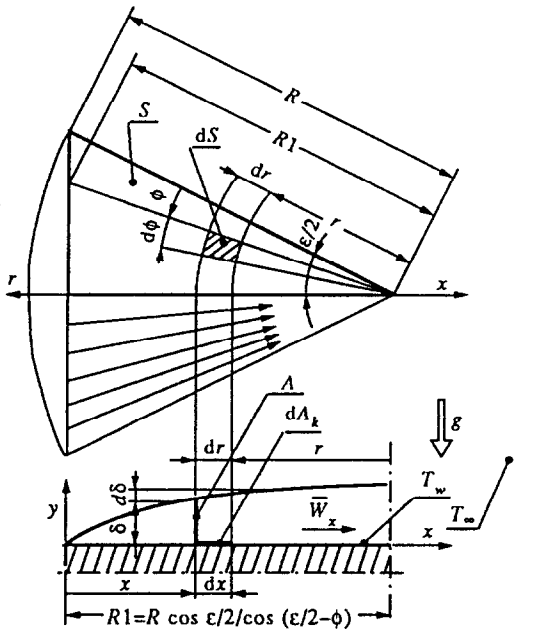

FIG. 3. Physical concentric model of convective heat transfer from a fragment of triangular form of considered heated isothermal surface.

$$\overline{Nu}_R = \frac{3.256 \cdot Ra_R^{1/5}}{R \sin(\varepsilon)} \cdot \int_0^{\varepsilon/2} \cdot \int_0^{R1} \frac{r^{4/3}}{(R1^{7/3} - r^{7/3})^{1/4}} \cdot dr \cdot d\phi. \quad (23)$$

The solution of integral in equation (23) is

$$\int_0^{R1} \frac{r^{4/3}}{(R1^{7/3} - r^{7/3})^{1/4}} \cdot dr = \frac{4}{7} \cdot \left[\frac{R \cdot \cos(\varepsilon/2)}{\cos(\varepsilon/2 - \phi)}\right]^{7/4}. \quad (24)$$

Introducing (24) into (23) gives

$$\overline{Nu}_R = \frac{1.860 \cdot Ra_R^{1/5}}{\sin(\varepsilon)} \cdot \int_0^{\varepsilon/2} \frac{\cos^{7/4}(\varepsilon/2)}{\cos^{7/4}(\varepsilon/2 - \phi)} \cdot d\phi,$$

$$\overline{Nu}_D = \frac{2.455 \cdot Ra_D^{1/5}}{\sin(\varepsilon)} \cdot \int_0^{\varepsilon/2} \frac{\cos^{7/4}(\varepsilon/2)}{\cos^{7/4}(\varepsilon/2 - \phi)} \cdot d\phi. \quad (25)$$

The integral in Nusselt–Rayleigh relation (25) can be solved numerically only.

For the limiting case—round plate—the solution of the concentric model of the fluid flow is quasi the same as for the parallel model (relation (19))

$$Nu_R = 0.930 Ra_R^{1/5} \quad \text{or} \quad Nu_D = 1.227 Ra_D^{1/5}. \quad (26)$$

Instead of the diameter (D) of the circle circumscribing the polygon, one can use the diameter (d) of the circle inscribed in the polygon as the characteristic linear dimension. Because the relation between

these two dimensions is $D = d/\cos(\varepsilon/2)$, it implies that

$$Nu_d = C_D \cdot Ra_d^{1/5} \cdot \cos^{2/5}(\varepsilon/2) = C_d \cdot Ra_d^{1/5}, \quad (27)$$

where $C_D = Nu_D/Ra_D^{1/5}$.

For the model of fluid flow with parallel stream lines $C_D = 1.228/\cos^{2/5}(\varepsilon/2)$, according to equation (17) and from equation (28) it is obvious that $C_d = 1.228 = \text{const.}$

For the model with concentric stream lines $C_d = 1.228$ is valid for round horizontal plates only, because $D = d$.

VERIFICATION OF THE ANALYTICAL SOLUTION

Results obtained for a round horizontal plate (equation (19)) or for a square plate can be compared with theoretical and experimental results published by other authors. About the other shapes of heating plates (triangle, pentagon, hexagon...) no information has been found. Because of the differences between the characteristic lengths in Nusselt–Rayleigh relations the results could not have been directly compared. Due to this, some of the dimensionless equations describing the convective heat transfer from a horizontal isothermal plate have been recalculated using the diameter as the characteristic length.

The solution presented by Rotem and Claassen [1] for an infinite plate of a length of ($L = D/2$) and for ($Pr \gg 1$) is

$$Nu_L = 0.767 \cdot Ra_L^{1/5}, \quad Nu_D = 1.012 \cdot Ra_D^{1/5}. \quad (28)$$

Goldstein and Lau [13] used ($a = A/P = D/4$), as the characteristic length, where A is the area, P is the perimeter and D is the diameter of the heat transferring surface. The numerical solution obtained by them for ($Pr = 0.7$) is

$$Nu_a = 0.621 \cdot Ra_a^{1/5}, \quad Nu_D = 1.081 \cdot Ra_D^{1/5}. \quad (29)$$

Experimental results obtained by the same authors for square naphthalene plates in air ($10 < Ra_a < 4.8 \times 10^3$) have the form

$$Nu_a = 0.746 \cdot Ra_a^{1/5}, \quad Nu_D = 1.299 \cdot Ra_D^{1/5}. \quad (30)$$

Experimental and theoretical results of convective heat transfer from rings with adiabatic plug published by Lewandowski *et al.* [8], expressed by Nusselt–Rayleigh relations, for the boundary case—horizontal isothermal disk—are

$$Nu_D = 1.229 \cdot Ra_D^{1/5} \quad \text{theory}, \quad (31)$$

$$Nu_D = 1.127 \cdot Ra_D^{1/5} \quad \text{experiment}. \quad (32)$$

A thin-layer approximation of an analytical–numerical solution of the natural convection above an isothermal heated disk of a diameter (D), obtained by Robinson and Liburdy [14] for ($Pr = 0.72$), is

$$Nu_D = 0.982 \cdot Gr_D^{1/5}, \quad Nu_D = 1.049 \cdot Ra_D^{1/5}. \quad (33)$$

Results of experimental study of heat transfer from an isothermal round plate approximated by Lewandowski *et al.* [15] with the use of exponent (1/4) can be approximated also with the use of exponent (1/5)

$$Nu_D = 0.711 \cdot Ra_D^{1/4} \quad \text{or} \quad Nu_D = 1.127 \cdot Ra_D^{1/5}. \quad (34)$$

Al-Arabi and El-Riedy performed an experimental study of natural convection from an isothermal plate of finite size (square, rectangular and circular) with the use of the condensation method [6]. Their exponents were (1/4) for the laminar and (1/3) for the turbulent range. For the Rayleigh number values close to $Ra = 10^5$ experimental points may be also approximated by the dependence with the exponent (1/5). The result of recalculation is

$$Nu_D = 0.70 \cdot Ra_D^{1/4} = 1.245 \cdot Ra_D^{1/5}. \quad (35)$$

There is no information in the literature of free convection from horizontal triangular and hexagonal surfaces so the comparison of the solution of convective heat transfer from polygons, with the solutions of other authors, equations (28)–(35), is limited to horizontal round, square or rectangular plates. This comparison shows that all results of other authors recalculated to the linear dimension (D) used in this work, fall within a $-(7.2$–$27.7\%)$ range. Hence it may be stated, by analogy, that the solution suggested in this paper is correct not only for the round, square and rectangular horizontal plate, but also for other polygonal forms of heating/cooling surfaces.

EXPERIMENTAL PROCEDURE

The experimental apparatus was a Plexiglas tank. The main dimensions of the tank were 0.4 m in diameter and 0.5 m in height. Horizontal heating plates of different shapes were fixed on the tank bottom. All tested plates (triangular, square, hexagonal and circular) were of diameter $d = 0.07$ m, which is the diameter of the circle inscribed in the plate. Each heating plate had a layer structure and consisted, from the bottom, of polyurethane foam (heat insulator), lead plate (ballast), and flat electric heater covered by the heating plate. The heating plate also had the layer structure consisting of three parallel plates, two copper plates with bakelite layer between them.

The heat flux from the heater inside the device was transported through the bakelite layer between copper plates by conduction. Three thermocouples were used to measure the temperature of the upper copper plate and three of the lower copper surfaces. Each thermocouple was soldered into holes with the tips about 0.001 m from the copper–bakelite interface. Four thermocouples were used to measure the bulk temperature of the fluid (dehydrated glycerin) at different levels in the tank. The inaccuracy of the temperature measurement did not exceed ± 0.1 K. Establishment of different steady states was made by a cooling system located at the top of the tank. This

sytem consisted of a copper coil connected to a thermostat.

During experimental runs the surface temperatures of the heating plate, at three points of lower and upper heating surfaces, bulk temperature of the fluid and the voltage (U) and current (I) of the heater inside the heating plate were measured. All these data were recorded during established steady states. Steady state was assumed to have been reached when the e.m.f. reading varied by less than 3 μV over a 10 min period. Details on the setup and on experimental procedure is given in refs. [10–12].

For the purpose of flow visualization two methods were employed. The first of them had a light-sheet and aluminum powder suspended in glycerine serving as tracer particles. In the second method of visualization the coloring agent from indelible pencil in the form of cylinders of 0.5 mm in diameter and of 0.5 mm height were stuck along the leading edges of plates tested. Water was used as a tested fluid in the second method.

Experiments were carried out in an hermetically closed vessel using dehydrated glycerin as the test fluid. The density, thermal expansion coefficient and dynamic viscosity of the liquid were experimentally determined after each experimental run. The thermal conductivity of the liquid was taken from the published data.

The heat flux density transferred through the heating plates was calculated according to formula:

$$q = (\lambda/h)(T_L - T_U), \tag{36}$$

where λ is the thermal conductivity of the heating plate of sandwich structure at the characteristic temperature ($T_{ch} = (T_U + T_L)/2$), $h = 2.72$ mm is the thickness of the plate and T_U and T_L are the average temperatures of upper and lower surfaces of the heating plate.

The correlation of thermal conductivity (λ) vs characteristic temperature (T_{ch}) for heating plates (36) was estimated experimentally on a special stand constructed especially for this purpose and is:

$$\lambda = 0.21036 + 8.092 \times 10^{-4} \cdot T_{ch}. \tag{37}$$

EXPERIMENTAL RESULTS

Using the least square method the experimental points obtained for various shapes of plates tested are correlated by Nusselt–Rayleigh relations:

$$Nu_D = 1.760 \cdot Ra_D^{1/5} \quad \text{triangle}, \tag{38}$$

$$Nu_D = 1.512 \cdot Ra_D^{1/5} \quad \text{square}, \tag{39}$$

$$Nu_D = 1.515 \cdot Ra_D^{1/5} \quad \text{hexagon}, \tag{40}$$

$$Nu_D = 1.267 \cdot Ra_D^{1/5} \quad \text{disk}. \tag{41}$$

Experimental results presented in the form of average Nusselt numbers (Nu_D) vs Rayleigh numbers (Ra_D) are shown in Figs. 4–7.

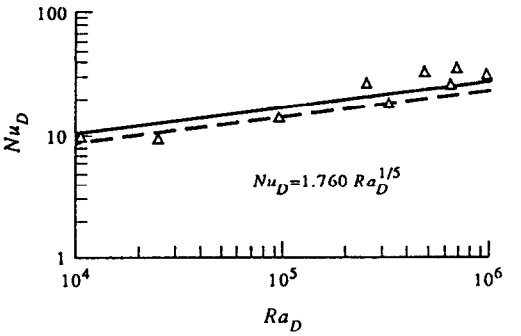

FIG. 4. Experimental data (points) for an equilateral triangle compared with the theoretical result. Solid line represents solution of the model with parallel stream lines and dashed line the solution of the model with concentric stream lines.

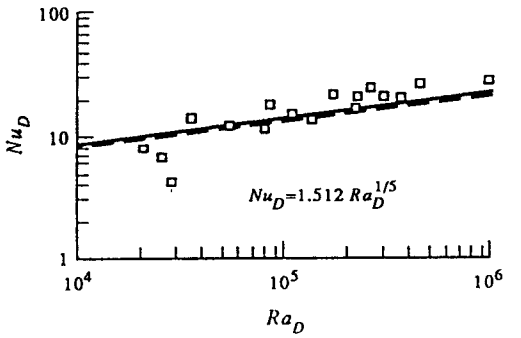

FIG. 5. Experimental data (points) for square surface compared with the theoretical result. Solid line represents solution of the model with parallel stream lines and dashed line the solution of the model with concentric stream lines.

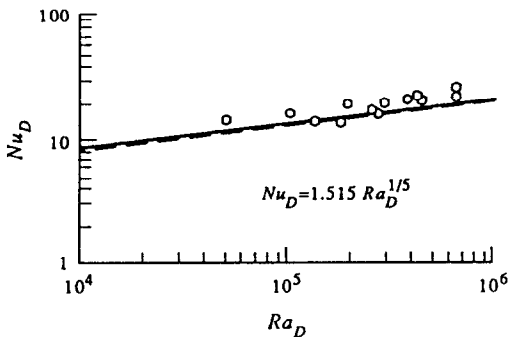

FIG. 6. Experimental data (points) for a regular hexagonal surface compared with the theoretical result. Solid line represents solution of the model with parallel stream lines and dashed line the solution of the model with concentric stream lines.

Recalculation of experimental results with the use of the diameter of the circle inscribed in polygon (d) as the characteristic length, leads to correlation:

$$Nu_d = 1.337 \cdot Ra_d^{1/5}. \tag{42}$$

This relation, as can be seen from Fig. 8, is valid for all shapes of plates tested.

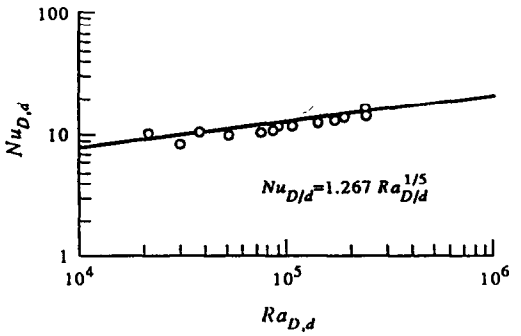

FIG. 7. Experimental data (points) for a round surface compared with the theoretical result (line).

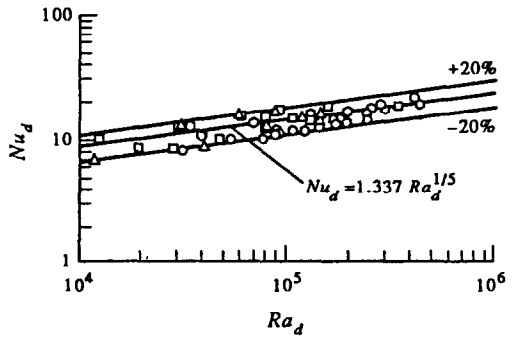

FIG. 8. Experimental results recalculated with the use of diameter of the circle inscribed in polygon (d) as the characteristic linear dimension.

Experimental results (points) plotted in the form of $C_D = Nu_D/Ra_D^{1/5}$ (Fig. 9(a)) or $C_d = Nu_d/Ra_d^{1/5}$ (Fig. 9(b)) vs ε were compared with the analytical solution of the parallel model (17) (solid lines) and of the concentric model of the flow pattern (27) (dashed lines) in Fig. 9.

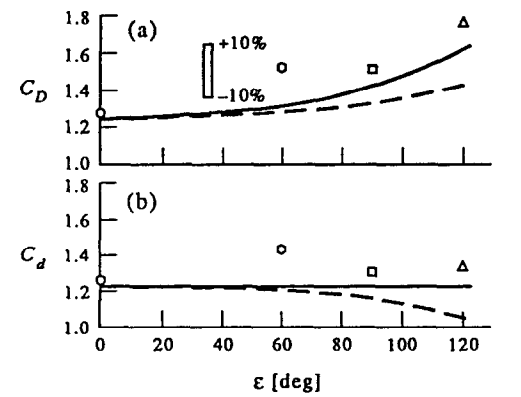

FIG. 9. Comparison of the analytical solution of the parallel model (solid line) and the concentric model (dashed lines) with experimental results (points); (a) the diameter of the circle circumscribed on polygonal surface (D) is the characteristic linear dimension, (b) the diameter of the circle inscribed in polygonal surface (d) is the linear dimension.

Table 1.

Model	Angle (shape) $\varepsilon = \pi/3$ (triangle)	$\varepsilon = \pi/4$ (square)	$\varepsilon = \pi/6$ (hexagon)	$\varepsilon \Rightarrow 0$ (disk)
Parallel	1.620	1.410	1.301	1.228
Concentric	1.357	1.296	1.256	1.227
Experiment	1.760	1.512	1.515	1.267

In Table 1 comparison of solutions of models with parallel stream lines (18) and with concentric stream lines (25), in the form of $C_D = Nu_D/Ra_D^{1/5}$, for triangular ($\varepsilon = \pi/3$), square ($\varepsilon = \pi/4$), hexagonal ($\varepsilon = \pi/6$) and round plate ($\varepsilon \Rightarrow 0$), together with experimental results have been presented.

In Table 2 theoretical results and experimental data recalculated, according to relation (27), with the use of the diameter (d) of the circle inscribed, as characteristic linear dimension, have been presented as $C_d = Nu_d/Ra_d^{1/5}$.

RESULTS OF VISUALIZATION OF NATURAL CONVECTION FROM POLYGONS

Results of visual research were obtained on horizontal isothermal hexagonal, square and triangular plates. All tested plates were of the same diameter $d = 0.07$ m of the circle inscribed in them. From many photographs of heat fluxes, the cases of $Q = 16.5$ W (Fig. 10(a)) and of $Q = 36.2$ W (Fig. 10(b)) have been chosen as an example for presentation.

CONCLUSIONS

The suggested models of the free convective heat transfer from isothermal, horizontal plates of different shapes exhibit an agreement with results of experimental investigations which cannot be only accidental.

Theoretical and experimental results presented in this paper are in good agreement.

From the analysis of visual experiments it is obvious that for the triangular plate the fluid flow is similar to that of the model of parallel flow pattern; in the case of a square plate both models give results of nearly the same magnitude; for a hexagon plate the model

Table 2.

Model	Angle (shape) $\varepsilon = \pi/3$ (triangle)	$\varepsilon = \pi/4$ (square)	$\varepsilon = \pi/6$ (hexagon)	$\varepsilon \Rightarrow 0$ (disk)
Parallel	1.228	1.228	1.228	1.228
Concentric	1.028	1.128	1.186	1.227
Experiment	1.334	1.315	1.433	1.267

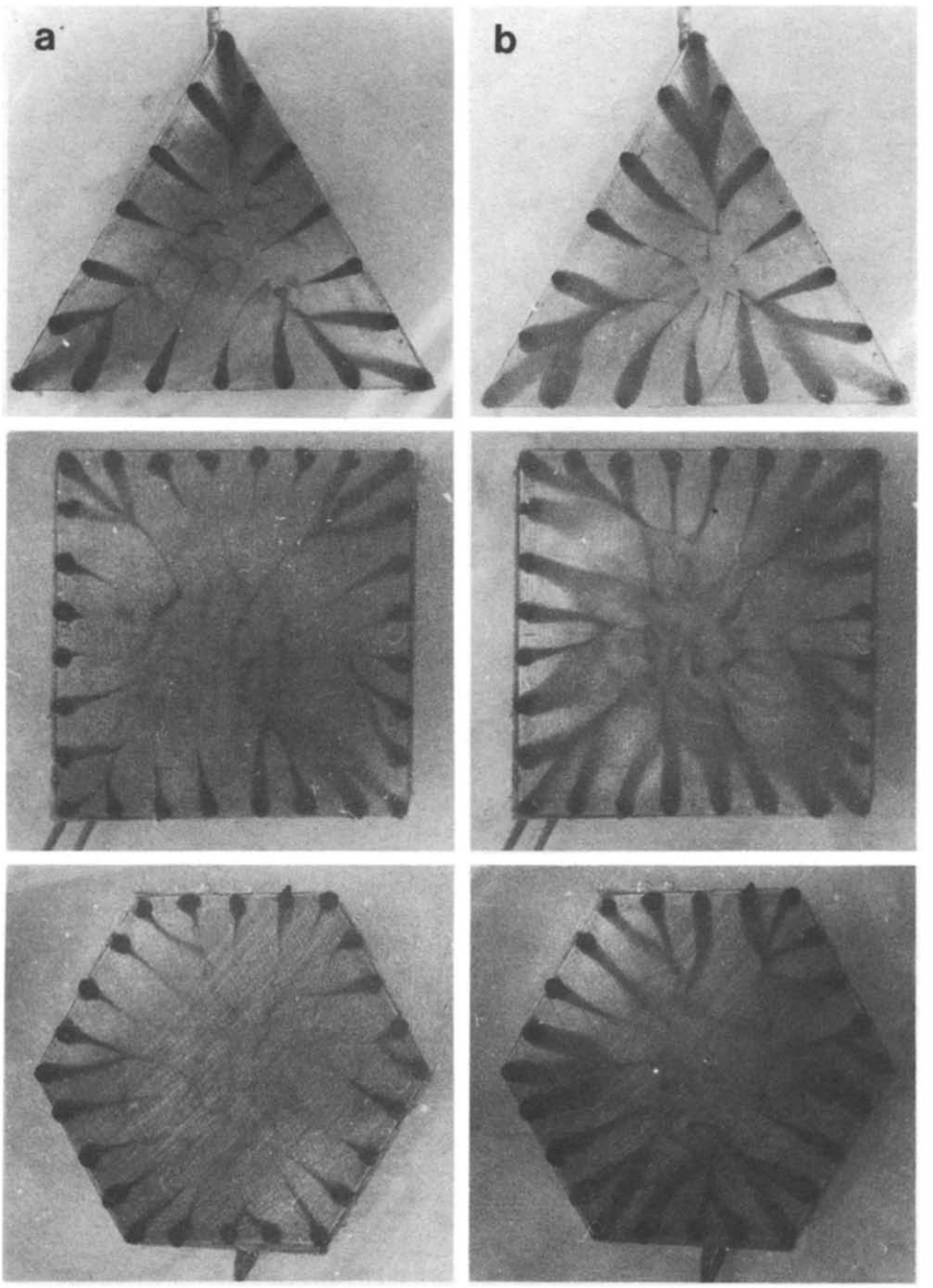

FIG. 10. Photographs of stream lines existing during the natural convection heat transfer experiment from horizontal isothermal triangle, square and hexagon, where heat fluxes are: (a) 16.5 W and (b) 36.2 W. Tested fluid is water.

of concentric fluid motion seems to prevail over that of the parallel model.

The other comparison of theoretical and experimental results suggests that the real free convective fluid flow above polygons follows a mechanism which is similar to that of the model of parallel stream lines.

In this work the theoretical consideration is based, for both models, on the solution of simplified Navier–Stokes equations obtained for plane flow and expressed as velocity relation (2). It is probable, that for the concentric model of the fluid flow the solution of velocity relation, obtained for cylindrical coordinates, would give results of better agreement with visual experimental data. These data indicate that free convective heat transfer is of complex nature and follows a mechanism which is between two boundary cases, concentric and parallel.

Both proposed models and their simplified solu-

tions, are merely the first approximation to the real phenomenon. It is very likely that this study would inspire other investigators. The solution of the simultaneous partial differential equations in cylindrical coordinates as well as further experimental studies would give more information and a better description of the phenomenon.

REFERENCES

1. Z. Rotem and L. Claassen, Natural convection above unconfined horizontal surfaces, *J. Fluid Mech.* **38,** 173–192 (1969).
2. W. Schneider, A similarity solution for combined forced and free convection flow over a horizontal plate, *Int. J. Heat Mass Transfer* **22,** 1401–1406 (1979).
3. F. F. Ling, Free convection and free-and-forced convection above a horizontal flat surface, *Int. J. Mech. Ing. Edu.* **15,** 10–14 (1985).
4. A. K. Chellappa and P. Singh, Possible similarity formulations for laminar free convection on a semi-infinite horizontal plate, *Int. J. Engng Sci.* **27**(2), 161–167 (1989).
5. P. Singh and K. A. Narayan, Free convection heat transfer over horizontal plate at low Prandtl number, *Can. J. Chem. Engng* **67,** 507–512 (1989).
6. M. Al-Arabi and M. El-Riedy, Natural convection heat transfer from isothermal horizontal plates of different shapes, *Int. J. Heat Mass Transfer* **19,** 1399–1414 (1976).
7. M. Miyamoto, Y. Katoh, J. Kurima, S. Kurihara and K. Yamashita, Free convection heat transfer from vertical and horizontal short plates, *Int. J. Heat Mass Transfer* **28,** 1733–1745 (1985).
8. W. M. Lewandowski, P. Kubski and J. M. Khubeiz, Laminar free convection heat transfer from horizontal ring, *Wärme und Stroffübertragung* (submission to publication).
9. W. M. Lewandowski, Natural convection heat transfer from plates of finite dimensions, *Int. J. Heat Mass Transfer* **34,** 875–885 (1991).
10. W. M. Lewandowski, H. Bieszk and P. Kubski, Experimental study of natural convective heat transfer from horizontal isothermal triangle, square, hexagon and disc, *Inz. Chem. i Proces.* **4,** 505–517 (1993).
11. W. M. Lewandowski, P. Kubski and H. Bieszk, Theoretical considerations on convective heat transfer from horizontal, isothermal triangle, square and hexagon, *Archiwum Termodyn.* (in press).
12. W. M. Lewandowski, H. Bieszk and P. Kubski, Free convection heat transfer from polygonal horizontal surface. *11th Congress of Chem. Engng CHISA* (1993).
13. R. J. Goldstein and K. S. Lau, Laminar natural convection from a horizontal plate and the influence of plate-edge extensions, *J. Fluid Mech.* **129,** 55–75 (1983).
14. S. B. Robinson and J. A. Liburdy, Prediction of the natural convective heat transfer from a horizontal heated disk, *J. Heat Transfer, Trans. ASME* **109,** 906–911 (1987).
15. W. M. Lewandowski, H. Bieszk and J. Cieśliński, Influence of cylindrical screens on free convection heat transfer from a horizontal plate, *Int. J. Heat Fluid Flow* **12,** 91–94 (1991).

APPENDIX A

Equation (14), given once more as (43) is a second order differential equation and its solution is based on two boundary conditions.

$$\delta \cdot \mathrm{d}(\delta^3 \cdot \mathrm{d}\delta/\mathrm{d}x) = \frac{432 \cdot R^3}{Ra} \cdot \mathrm{d}x. \tag{43}$$

The first condition is an assumption that the solution is a family of exponential curves

$$\delta = \delta_0 \cdot x^n. \tag{44}$$

The second boundary condition is:

$$\delta = 0 \quad \text{for } x = 0. \tag{45}$$

Differentiation of equation (44) leads to

$$\mathrm{d}\delta/\mathrm{d}x = \delta_0 \cdot n \cdot x^{n-1}. \tag{46}$$

Introducing equation (46) into equation (43) one obtains

$$\delta_0 \cdot x^n \cdot \mathrm{d}(\delta_0^3 \cdot x^{3n} \cdot \delta_0 \cdot n \cdot x^{n-1}) = \frac{432 \cdot R^3}{Ra} \cdot \mathrm{d}x, \tag{47}$$

$$n \cdot \delta_0^5 \cdot x^n \cdot \frac{\mathrm{d}}{\mathrm{d}x}[x^{4n-1}] = \frac{432 \cdot R^3}{Ra}. \tag{48}$$

Differentiation of equation (48) leads to

$$n \cdot (4 \cdot n - 1) \cdot \delta_0^5 \cdot x^{5n-2} = \frac{432 \cdot R^3}{Ra}. \tag{49}$$

The relation (49) is true for ($n = 2/5$) and

$$\delta_0 = \frac{4.478 \cdot R^{3/5}}{Ra^{1/5}} \tag{50}$$

and next (δ) is

$$\delta = \frac{4.478 \cdot R^{3/5}}{Ra^{1/5}} \cdot x^{2/5}. \tag{51}$$

APPENDIX B

The case of pure concentric fluid flow takes place during free convective heat transfer process from a horizontal round plate. The solution of equation (20), based on this model case, is presented below.

Equation (20) rewritten as equation (52) is:

$$\frac{\delta}{r}\frac{\mathrm{d}}{\mathrm{d}r}[r\delta^3(-\mathrm{d}\delta/\mathrm{d}r)] = \frac{432 \cdot R^3}{Ra}. \tag{52}$$

Using typical methods of solution of second order differential equations the final result has not been obtained. For subsequent considerations one can assume, in pursuance of ref. [9], that the mean increase of the boundary layer thickness along the path of its growth, equation (53), is constant.

$$\frac{\mathrm{d}\delta}{\mathrm{d}r} = \frac{\overline{\mathrm{d}\delta}}{\mathrm{d}r} \cong \text{idem}. \tag{53}$$

Introduction of equation (54) into equation (52) and differentiation of equation (52)

$$F = \left|\frac{\overline{\mathrm{d}\delta}}{\mathrm{d}r}\right| \quad \text{and} \quad K = \frac{432 \cdot R^3}{Ra \cdot F} \tag{54}$$

yields to the first order differential equation and next to

$$\frac{\delta}{r}\left[r \cdot 3\delta^2 \cdot \frac{\mathrm{d}\delta}{\mathrm{d}r} + \delta^3\right] = -K \tag{55}$$

or

$$3\delta\frac{\mathrm{d}\delta}{\mathrm{d}r} + \frac{\delta^4}{r} = -K. \tag{56}$$

The equation (56) is a non-homogeneous differential equation

$$\frac{3}{4}\frac{\mathrm{d}u}{\mathrm{d}r} + \frac{u}{r} = -1 \tag{57}$$

where

$$u = \delta^4/K. \tag{58}$$

The solution of equation (57) for round plate with following boundary condition (for $r = R$ (leading edge) $\delta = 0$

and $u = 0$) is

$$u = \frac{4}{7} \cdot \frac{(R^{7/9} - r^{7/9})}{r^{4/9}} \tag{59}$$

and next

$$\delta = \frac{A}{F^{1/4}} \cdot \frac{(R^{7/9} - r^{7/9})^{1/4}}{r^{1/9}} \tag{60}$$

where

$$A = \frac{3.964 \cdot R^{3/4}}{Ra^{1/4}}. \tag{61}$$

The value of the coefficient (F) may, however, be determined according to its definition (53) from differentiation of equation (60)

$$\frac{\mathrm{d}\bar{\delta}}{\mathrm{d}r} = \frac{1}{S} \cdot \int_0 \frac{\mathrm{d}\delta}{\mathrm{d}r} \mathrm{d}s = \frac{1}{\pi R^2} \cdot \int_0^{\varepsilon = 2\pi} \int_0^R r \frac{\mathrm{d}\delta}{\mathrm{d}r} \mathrm{d}r \, \mathrm{d}\varepsilon = \frac{2}{R^2} \int_0^R r \, \mathrm{d}\delta. \tag{62}$$

Since $r \, \mathrm{d}\delta = \mathrm{d}(r\delta) - \delta \, \mathrm{d}r$, equation (62) is

$$F = \frac{2A}{F^{1/4} \cdot R^2} \cdot \int_0^R \frac{(R^{7/3} - r^{7/3})^{1/4}}{r^{1/3}} \mathrm{d}r. \tag{63}$$

The value of the integer in equation (63) is

$$\int_0^R \frac{(R^{7/3} - r^{7/3})^{1/4}}{r^{1/3}} \mathrm{d}r = 1.378 \cdot R^{2.3}. \tag{64}$$

Substitution of equations (64) and (61) into equation (63) gives

$$F^{1/4} = \frac{1.613}{R^{1/20}}. \tag{65}$$

The thickness of the boundary layer may be determined from substitution of equations (65) and (61) into equation (60)

$$\delta = \frac{2.454 \cdot R^{3/4} \cdot (R^{7/9} - r^{7/9})^{1/4}}{Ra^{1.5} \cdot r^{1/3}}. \tag{66}$$

This solution based on the model of concentric fluid flow on the round horizontal plate, where $R = \text{const.}$, has to be modified because of the triangular surface considered $R = Rl \neq \text{constant}$ (Fig. 3).